Iğdır Üniversitesi Fen Bilimleri Enstitüsü Dergisi, 13(3), 1888-1901, 2023
Journal of the Institute of Science and Technology, 13(3), 1888-1901, 2023

ISSN: 2146-0574, eISSN: 2536-4618

Chemistry **DOI: 10.21597/jist.1180016**

Research Article

Received: 26.09.2022 **Accepted: 18.05.2023**

To Cite: Yılmaz, M., Baykal, M., Farghaly, A.A. & Demir, M. (2023). Production of Porous Carbon by the Synergistic Chemical and Physical Activations and its Capacitive Performance**.** *Journal of the Institute of Science and Technology*, 13(3), 1888-1901.

Production of Porous Carbon by the Synergistic Chemical and Physical Activations and its Capacitive Performance

Murat YILMAZ[1*], Mikail BAYKAL[2], Ahmad A. FARGHALY[3], Müslüm DEMİR[4]

Highlights:

- Biomass-derived carbons have been investigated for supercapacitor applications
- Unique oxygen-rich porous carbons were successfully prepared by combining chemical KOH and physical CO_2 activation methods
- The resulting PC-4K-CO_2 porous carbon displayed a hierarchical porous structure with a high surface area of 1318.4 cm^2/g
- The highest specific capacitance of 151 F/g at a current density of 0.5 A/g in the 1 M KOH electrolyte
- PC-4K-CO_2 sample has achieved an excellent long-cycling life with only 8.6% loss of its initial capacitance over 500 cycles

ABSTRACT:

Biomass-derived carbons have been extensively investigated for supercapacitor applications thanks to their advantages such as high specific capacitance value, low cost, environmental friendliness, and readily available natural materials. In this study, unique oxygen-rich porous carbons were successfully prepared by combining chemical KOH and physical CO_2 activation methods. The physical and textural properties of as-prepared carbon materials are highly dependent on the synthesis conditions. The resulting PC-4K-CO_2 porous carbon exhibited a hierarchical porous structure consisting of micropores, mesopores, and macropores along with a large surface area of 1318.4 cm^2/g, which allowed high exposure of electrocatalytic sites and ion diffusion/transfer facilitated. As a supercapacitor electrode material, PC-4K-CO_2 porous carbon prepared at 800 °C with synergic activation of KOH and CO_2 showed the highest specific capacitance of 151 F/g at a current density of 0.5 A/g in the 1 M KOH electrolyte. Besides, the electrode prepared with the PC-4K-CO_2 sample has achieved an excellent long-cycling life with only an 8.6% loss of its initial capacitance over 500 cycles even at a current density of 5 A/g. The current study emphasizes the environmental significance of turning pistachio shells into electrode materials for high-performance supercapacitors.

Keywords:

- KOH activating
- Pistachio shell
- Supercapacitor
- Biochar
- Physical activating

[1]Murat YILMAZ (**Orcid ID:** 0000-0002-6465-6960), Osmaniye Korkut Ata University, Bahce Vocational School, Department of Chemistry and Chemical Processing Technologies, Osmaniye, Türkiye

[2]Mikail BAYKAL (**Orcid ID:** 0000-0001-6919-9052), Osmaniye Korkut Ata University, Faculty of Engineering, Department of Chemical Engineering, Osmaniye, Türkiye

[3]Ahmad A. FARGHALY (**Orcid ID:** 0000-0001-7948-3700), Chemical Sciences and Engineering Division, Argonne National Laboratory, Lemont, Illinois, United States

[4]Müslüm DEMİR (**Orcid ID:** 0000-0001-6842-8124), Osmaniye Korkut Ata University, Faculty of Engineering, Department of Electrical and Electronics Engineering, Osmaniye, Türkiye

Corresponding Author: Murat YILMAZ, e-mail: muratyilmaz@osmaniye.edu.tr

This study was produced from Mikail BAYKAL's Master's thesis.
The article was held in Konya on 10-11 June 2021 at the "14. Presented orally at the National Chemical Engineering Congress (UKMK 2020).

INTRODUCTION

In recent years, supercapacitors have attracted much attention because of their long service life, cycle performance, high specific capacitance, fast charging and discharging rate, ease of maintenance, and safe operation (Zhang et al., 2016; Zhao et al., 2018). The supercapacitor has the dual function of secondary batteries and traditional capacitors. Compared to ordinary batteries, supercapacitors have a higher power density, and they bridge the gap between these two traditional technologies since their energy density is substantially higher than conventional capacitors (Zhao et al., 2010; Gao et al., 2013; Du et al., 2018). Depending on the charge storage technique, supercapacitors are categorized as electric double-layer capacitors (EDLCs) and pseudocapacitors (Miller and Simon, 2008; Inagaki et al., 2010). In pseudocapacitors, the energy is stored by a faradaic reaction on the surface of the active materials, whereas in EDLCs, electrical charges are accumulated on the electrode at the electrolyte interface (Zhang et al., 2019). Porous carbons (PCs), graphene, and carbon nanotubes as promising electrode materials for electric double-layer capacitors have been actively explored due to their high surface area, non-toxicity, controllable porosity, various forms of usability, and excellent electronic conductivity (Seyedeh et al., 2021; Zhang et al., 2021). It has been observed that biomass-derived porous carbon has emerged as the most prominent electrode material for supercapacitors due to its large pore volume, high surface area, tunable surface functionality, and low production cost (Zhang and Zhao 2009; Yu et al., 2018).

The selection of the raw biomass precursor and the activation process is highly decisive for the surface chemical properties and microstructures of the resulting porous carbon. The utilization of waste biomass materials in the preparation of carbon-based electrodes for electrochemical applications is still in its infancy (Altay et al., 2021; Zhong et al., 2021). Many biomass resources have been studied as precursors for porous carbon products such as lignin, cellulose, peanut shell, etc. Biomass resources vary in microstructure, composition, nature of the connection between different components, and structure of each component (Ashourirad et al., 2018; Zhan et al., 2021). Pistachio shell is a by-product of pistachio production in factories and its annual production is 7.44 million tons worldwide. It is a clean, abundant, low-cost, and renewable source of biomass, which makes it a viable candidate as a raw material in the production of biomass-derived carbon-based materials (Duan et al., 2014; Chen et al., 2017; Demir et al., 2018; Altinci and Demir, 2020). In addition, since pistachio shells have low ash content, they are preferred over fossil raw materials in porous carbon production (Guo et al., 2019; Li et al., 2019).

It is viable to produce higher capacitive performance supercapacitors by tweaking the physicochemical properties of activated carbons. Physical and/or chemical activation methods are frequently employed in the preparation of carbon-based electrode materials for supercapacitors (Williams and Reed, 2006; Girgis et al., 2011; Wei et al., 2018). Physical activation takes place by first carbonizing the feedstock under an inert atmosphere and then activating it at high temperatures using steam (Liang and Wu, 2021) or CO_2 gas (Choudhury et al., 2021) as the activating reagent. Although the physical activation strategy has many merits, such as ease of preparation, environmental friendliness, low cost, and tunable pore formation. However, it suffers from the insufficient textural properties of the final carbons. Chemical activation, on the other hand, is accomplished by treating the carbon precursor with an activating agent such as $ZnCl_2$, KOH, or H_3BO_3. Chemical activation is a cost-effective process that has been utilized to produce porous carbons with high-performance textural properties. Nevertheless, it is accompanied by numerous issues, including the use of corrosive activating reagents and the need for complicated post-treatment processes, which have drastically

restricted its practical utilization (Ahmadpour and Do, 1996; Fan et al., 2004; Zhang et al., 2004). Thus, combining the physical and chemical activation methods will improve the properties of the produced carbons and allow for the design of advanced carbon electrodes. To the best of our knowledge, there have been few studies published in the literature on the fabrication of carbon-based electrode materials for supercapacitors synthesized through simultaneous physical and chemical activation. Here, high-performance carbon-based electrode materials for supercapacitors have been created using a unique synthesis method that uses simultaneous physical and chemical activation to create porous carbons.

In this study, we demonstrated the successful synthesis of porous carbons from pistachio shells using both chemical KOH activation and physical CO_2 activation in a single-step process. While the activation of pistachio shell with KOH has been carried out in many studies in the literature, the fact that KOH and CO_2 are carried out together in this study reveals the originality of our study. It has been found that the ratio of KOH to biochar and CO_2 environment have a significant impact on the produced porous carbons properties. The pore size distribution, morphology, crystal structure, and specific surface area of the prepared porous carbons were examined in depth. As a supercapacitor electrode material, porous carbons derived from pistachio shells via a simultaneous chemical KOH activation and physical CO_2 activation route demonstrated higher specific capacitance than carbons prepared solely through physical or chemical activation.

MATERIALS AND METHODS

Experimental

Materials

The pistachio shell (PS) used in this study was collected from the surrounding areas of Gaziantep province, Turkey. This kind of material includes cellulose, hemicellulose and lignin. Based on the literature carbon amount around 60%. Chemicals including KOH (95% purity) and HCl (37% purity) were purchased from Merck. 1-Methyl-2-pyrrolidinone (99% purity) and Poly (vinylidene fluoride) (PVDF) were purchased from Sigma-Aldrich. All of the chemical reagents used in the investigation were analytically pure and used straight from the container without further purification. All abbreviations used in this study are shown in Table S1.

Preparation of porous carbon from pistachio shell waste (AC-PS)

The synthesis of porous carbon was carried out in the following manner: first, the pistachio shell was washed with distilled water to eliminate surface impurities. The washed pistachio shell was dried in a 105 °C drying oven before being crushed to a particle size of less than 0.71 mm. Following that, 10 grams of ground shells and 80 mL of distilled water were placed in a 150 mL PPL stainless steel autoclave reactor. The hydrothermal carbonization (HTC) procedure was used to produce biochar, and it was completed at 180 °C for 4 hours. The autoclave reactor was allowed to cool down naturally to room temperature. Dry biochar was produced by filtering the reaction product, washing it with distilled water, and drying it for a day at 110 °C. To remove impurities from the resulting biochar, it was washed with 3.0 M HCl acid for 45 minutes under constant stirring before being filtered using vacuum filtration. This process was then repeated three times with distilled water, ethyl alcohol, and finally distilled water for 45 minutes each to remove the residual chemicals. The cleaned biochar was allowed to dry for one day at 110 °C. The biochar was mixed with KOH at a pistachio shell / KOH mass ratio of 1/0, 1/4, 1/5, and 1/6 while the total mass was kept at 2.0 g. The quartz boat containing the biochar-KOH mixture was placed in a tubular furnace through which N_2 gas was passed for activation. The biochar was heated to the activation temperature of 800 °C for 60 minutes at a heating rate of 10 °C

min^{-1} in a CO_2 environment in order to create the porous carbons. Based on the biochar: KOH ratio, as-prepared samples are denoted as PC-CO_2 (no KOH added, only biochar at a CO_2 atmosphere), PC-4K-CO_2 (1/4), PC-5K-CO_2 (1/5), and PC-6K-CO_2 (1/6). The same procedure was repeated for the sample in the N_2 atmosphere (wt. ratio of biochar/KOH of 1/4), and the as-prepared sample was donated as PC-4K-N_2. The synthesis of pistachio shell-derived porous carbons is shown schematically in Figure 1.

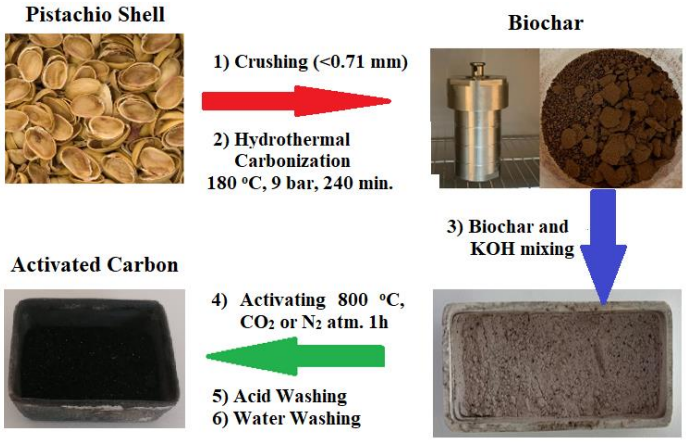

Figure 1. Schematic illustration of porous carbons synthesis

Characterization

To study the physical and morphological properties of the as-prepared porous carbon materials, the following characterization techniques have been implemented: scanning electron microscopy (SEM, ZEISS SIGMA 300) to identify the morphological characteristics, and X-ray diffraction (XRD, Panalytical Empyrean) to examine the phase purity. The specific surface area of the pistachio shell-derived porous carbon (Brunauer–Emmett–Teller (BET) theory-based measurement) was determined at 75.81K in $p/p^o = 0.2782$ using a surface area and porosity analyzer (BET Micromeritics 3 Flex). The samples' surface chemistry was determined using X-ray photoelectron spectroscopy (XPS, Specs-Flex XPS).

Electrochemical characterization

Using a three-electrode system, the CHI 660E, the electrochemical performance of produced porous carbon electrodes was evaluated at ambient temperature (CH Instruments). The electrochemical property of the porous carbon was measured with the help of an aqueous 1.0 M concentration of KOH electrolyte. A certain amount of polyvinylidene fluoride (PVDF) binder to be used in electrode preparation is taken and dissolved in N-methyl-2-pyrrolidone (NMP) solvent. The working electrode is synthesized by pressing a slurry of porous carbon derived from pistachio shell powder (85 wt.%) and polyvinylidene fluoride (PVDF, 15 wt.%) mixture onto a piece of nickel foam. To avoid unexpected effects, the prepared porous carbon paste was homogeneously and equally coated on each electrode (8 mg/cm^2) and then dried at 110 °C in an oven overnight. Finally, to create the functioning electrodes, each electrode was pressed at 10 MPa to a thick sheet. The reference electrode was an Ag/AgCl electrode (Argenthal, 3M KCl, 0.207V versus SHE at 25 °C), and the counter electrode was a piece of platinum gauze with an exposed area of 4 cm^2. The mass and area of the working electrode prepared from nickel foam are so important in calculating the specific capacitance of the electrode. The prepared porous carbon paste was coated on an effective surface area of approximately 1 cm^2 of the electrode. We tried to fully investigate the electrochemical parameters starting from -1 to 1. Based on our investigation we found the optimal potential window between 0.2 to 0.8. The current density for GCD measurements is modified from 0.5 to 30 A/g, and the 0.8 to 0.2 V voltage window is used for CV and GCD measurements. The scan speeds used for the CV measurement ranged from 10 to 500

mV/s. The frequency range for the impedance plots was 10^2 to 0.01 Hz, with an applied DC voltage of 0 V, and an amplitude of 5 mV rms. The GCD approach was used to conduct stability tests on the electrodes while maintaining a consistent current density of 0.5 mA cm^2 and the same potential window. Using GCD curves from Equation 1, the specific capacitance values in the three-electrode system were computed (Ahmadpour et al., 1998):

$$C = \frac{I*\Delta t}{m*a*\Delta V} \quad (1)$$

Where C represents the specific capacitance (F/g) of the electrode materials, Δt is the discharge time (s), I denotes the discharge current (A), m is the mass (g) of active material loaded, a (wt.%) refers to the mass percentage of the active substance and ΔV denotes the potential window (V) excluding IR drop.

RESULTS AND DISCUSSION

Physical Characterization

Morphology and size distribution

The SEM micrographs in Figure 2 and Figure S1 show the morphology of the as-prepared carbon samples as well as the prominent effect of the KOH mass ratio on their microstructure. Except for the more dense PC-CO_2 sample, all of the synthesized samples had similar morphology in terms of particle shape and size. All of the samples displayed a nonhomogeneous, sponge-like structure. This sponge-like feature allows the sample to have a wide variety of pore sizes and a high surface area. A closer examination of the SEM micrographs reveals more information about the microstructure of the prepared samples by comparing the SEM images of each sample at 1.00 KX and 5.00 KX magnification. Porosity formation, for example, is clearly visible in the high-magnification SEM micrographs collected at 5.00 KX. In comparison to the other porous carbon samples, the SEM images of the PC-CO_2 sample revealed the formation of a less porous structure with thick flakes forming the porous network and a lower number of pores. On the other hand, a more porous structure with thinner flakes forming the porous interconnected framework and a larger number of pores is obvious in the SEM images of the PC-4K-CO_2 sample, which was physically activated in a CO_2 environment and chemically activated with KOH. The effect of the physical activating agent CO_2 vs N_2 on the microstructure of the produced porous carbons was evaluated by comparing the SEM micrographs of the PC-4K-CO_2 and PC-4K-N_2 samples with the same KOH content. It is evident that the application of the CO_2 atmosphere in the physical activation process resulted in the formation of a more porous structure, as shown in Figure 2. The CO_2 creates better porosity formation than N_2 through high-temperature intercalation. CO_2 shows better activity for the formation of creativity for structure in the carbon bases. Also based on the molecular distance between CO_2 and N_2, N_2 has a low formation while CO_2 has a large amount of level. Furthermore, the effect of the chemical activating agent KOH concentration on the microstructure of the resulting porous carbons was investigated. It is demonstrated that as the KOH content increases, the porosity, the number of pores, and the specific surface area of the resulting carbon structures increase as well, as shown in Figure 2 and Figure S1 due to the erosion of the surface of the pistachio shell by KOH. The SEM images of PC-5K-CO_2 and PC-6K-CO_2 are given in Figure S1.

Determining the microstructure is extremely important for the design and development of porous carbon-based devices. Furthermore, the formation of an electric double layer is strongly dependent on the pore characteristics and specific surface area of the porous carbon structure (Ahmadpour et al., 1998; Kalyani and Anitha, 2013; Gandla et al., 2020). Despite the fact that micropores typically

account for more than 95% of the total surface area of most porous carbon materials (Huang et al., 2021). The pore size distribution in porous carbons and the ratio of micropores to mesopores are of great importance in supercapacitor applications. IUPAC classified the pores dispersed in activated carbons as "micropores" for pore sizes of less than 2 nm, "mesopores" for those between 2-50 nm, and "macropores" for those greater than 50 nm (Zhao et al., 2018).

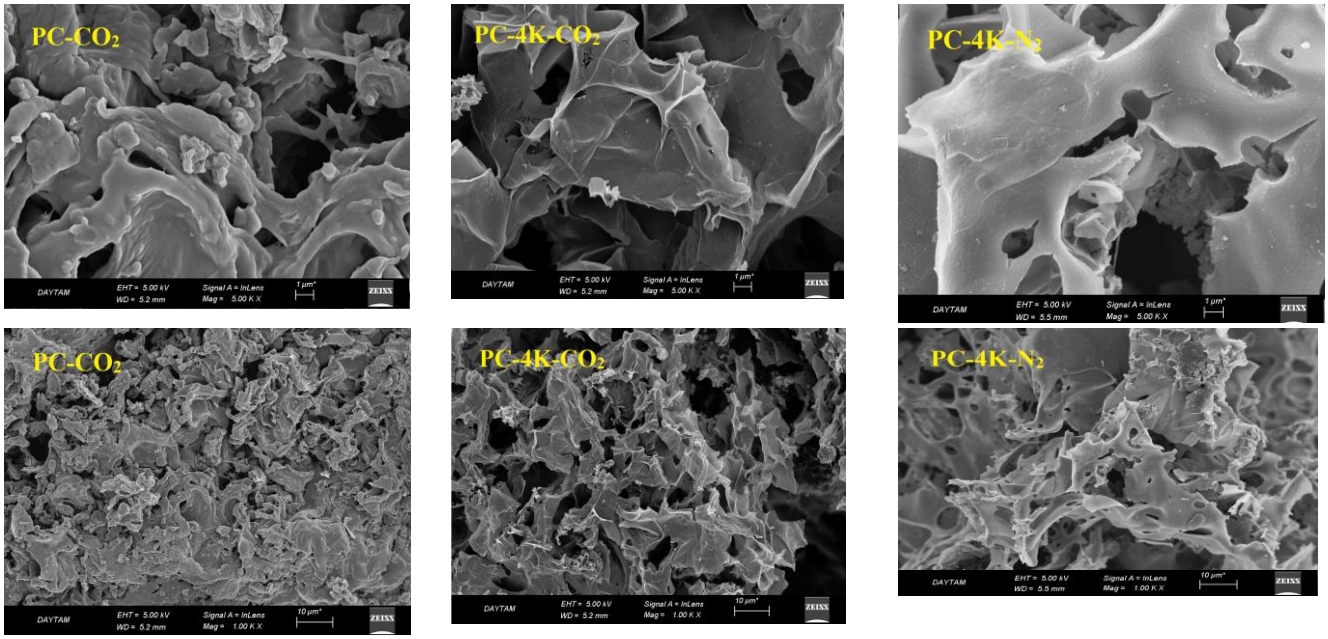

Figure 2. SEM micrographs of PC-CO_2, PC-4K-CO_2 and PC-4K-N_2 at different magnifications

Figure 3(a-b) illustrates how N_2 adsorption-desorption isotherms at 77 K for PC-CO_2, PC-4K-CO_2, and PC-4K-N_2 samples were used to assess the BET surface area, pore size distribution, and pore volume. The nitrogen adsorption-desorption isotherms of PC-5K-CO_2 and PC-6K-CO_2 carbon samples are given in Figure S2. All the prepared carbon samples displayed Type I and IV (according to the IUPAC classification) isotherm curves. The presence of microporosity is indicated by the sharp adsorption curve at a low relative pressure (0-0.1). A small hysteresis loop was observed at high relative pressures (0.4-0.8), indicating the presence of mesopores.

As shown in Figure 4, the pore size distribution calculated by the Barrett–Joyner Halenda (BJH) technique using the adsorption curve further confirms the presence of mesopores in the porous carbon structures obtained from the pistachio shells. At higher values of the relative pressures (> 0.8), there is no clear indication of the presence of macroporous. In addition, as seen in Figure 3(a), it is clearly obvious from the differences in the saturation adsorption of nitrogen curves of the carbon samples that the KOH activation agent significantly affects the pore structure of the porous carbons derived from the pistachio shell. Table 1 shows the textural properties of PC-CO_2, PC-4K-CO_2, PC-5K-CO_2, PC-6K-CO_2, and PC-4K-N_2 carbon samples. As shown in Table 1, the PC-CO_2 sample had a low surface area, pore volume, and porosity, whereas the other samples had a high N_2 sorption pore volume, with the PC-4K-N_2 sample having the highest value. The reasons behind those notable differences in the textural properties of as-prepared carbon samples are attributed to the nature of the activation process applied. For example, when only the CO_2 activation method was applied, a low porosity carbon framework was obtained, whereas when KOH activation was used, the surface area and pore volume were significantly increased due to the erosion effect of the KOH chemical activating agent on the carbon structure. Furthermore, when both CO_2 and KOH activation methods were applied, the textural properties of the as-prepared carbons were further improved due to their synergistic effect. More

prominently, when both physical and chemical activation methods were applied, the mesoporosity of the structure was clearly demonstrated.

The proposed synthesis mechanism for the formation of microporous-mesoporous carbon materials during the carbonization of pistachio shell-KOH mixtures at 800 °C in an environment of CO_2 includes the following steps. When the temperature of the tube furnace reaches 400 °C, the KOH is converted to K_2O, which combines with carbon to form K_2CO_3, and as the temperature further increases, K_2O is reduced to K. Potassium evaporates when the temperature of the tube furnace exceeds its boiling temperature (763 °C), and the produced potassium vapor permeates the carbon layers, causing micropores to develop in the carbon structure. Whereas the formation of mesopores in the resulting carbon structures could be attributed to the gasification of the micropores caused by the carbonate ions and etching of the exposed carbon atoms by oxygen atoms in the carbonate anion CO_3^{2-} in K_2CO_3 during the KOH activation process. Furthermore, KOH etches the carbonized pistachio shell ash, forming mesopores. As a result, porous carbons with both micropores and mesopores were produced by passing CO_2 gas through a tubular furnace containing pistachio shell-KOH mixtures at 800 °C. The phase purity and crystallographic structure of the produced PC-4K-CO_2 coded porous carbon sample was examined by X-ray diffraction (XRD) analysis. The XRD pattern of the PC-4K-CO_2 sample is given in Figure 3(c). The (002) and (100) planes of graphetic carbon are the two broad diffraction peaks at about 2Θ of 23° and 43°, respectively. The defective nature of the PC-4K-CO_2 sample, as well as the presence of amorphous and/or irregular carbon microdomains, was demonstrated by the shift of the (002) diffraction peak to lower angles when compared to pure graphite (23° vs. 26°). The low intensity and broadening of the measured diffraction peaks could be attributed to the high surface of the produced porous carbons by physical and chemical activation processes, which is in close agreement with the proposed activation mechanism.

Table 1. Physical properties and activation conditions of porous carbons prepared from pistachio shell

Porous carbons	Activation agent	S_{BET} (m^2/g)	$V_{pore(micro)}$ (cm^3/g)	$V_{pore(total)}$ (cm^3/g)
PC-CO_2	CO_2	166.8	0.25	0.27
PC-4K-CO_2	KOH and CO_2	1318.4	0.33	0.63
PC-4K-N_2	KOH	1184.0	0.43	0.53

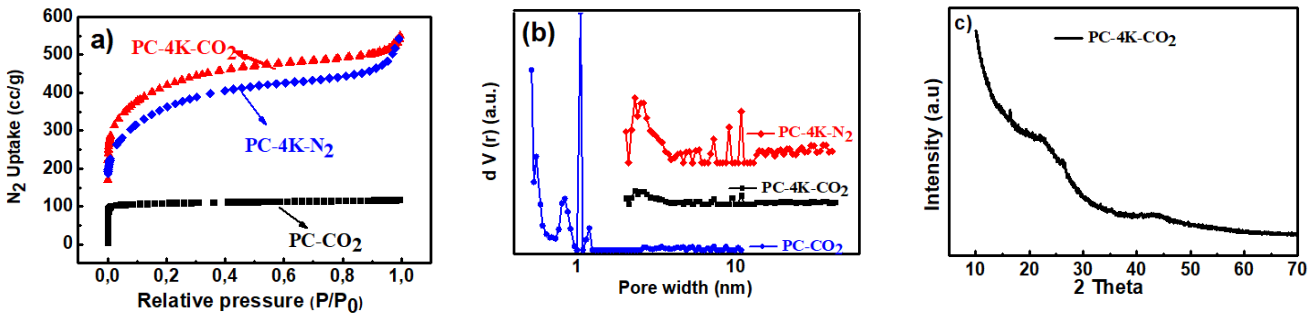

Figure 3. (a) Nitrogen adsorption-desorption isotherms of PC-CO_2, PC-4K-CO_2 and PC-4K-N_2 samples (b) Pore size distribution curves of PC-CO_2, PC-4K-CO_2 and PC-4K-N_2 samples (c) XRD diffraction pattern of PC-4K-CO_2 sample

The XPS has been applied to determine the surface configuration and chemical states of elements present in the PC-4K-CO_2 sample. The full-scan XPS of the PC-4K-CO_2 sample is presented in Figure 4(a) and reveals the high purity of the prepared porous carbon sample where only two main peaks of C1s (284.6 eV) and O1s (530.0 eV) were detected. Figure 4(b) illustrates the high-resolution C 1s spectrum of the PC-4K-CO_2 sample. One main and two relatively small peaks were detected. The main peak at 284.6 eV is assigned to -C=C, whereas the small peaks located at 285.3 eV and t 286.6

eV are attributed to the –C=O and –O-C=O, respectively (Kalyani and Anita, 2013; Zhong et al., 2021). Phenol and carbonyl oxygen functionalities have been found in the high-resolution O 1s spectrum of the PC-4K-CO_2 sample, Figure 4(c).

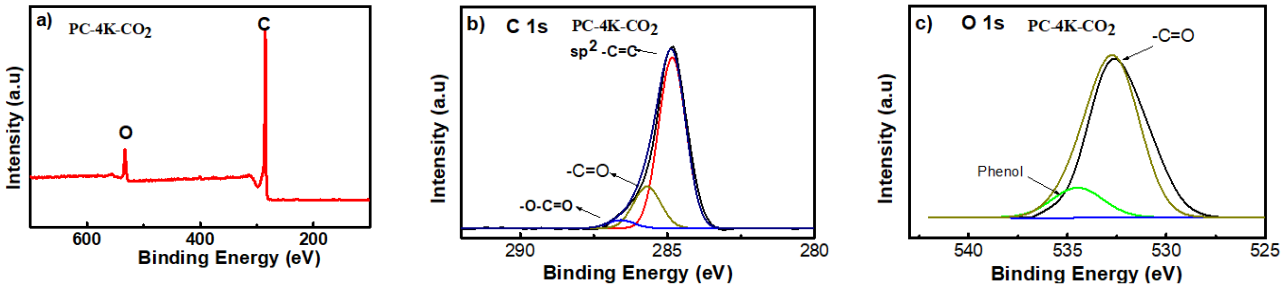

Figure 4. (a) XPS survey spectrum of PC-4K-CO_2 coded sample, (b) C 1s deconvoluted spectrum, (c) O 1s deconvoluted spectrum

Electrochemical characterization

The capacitive behavior of the pistachio shell-derived porous carbon electrodes was investigated in a three-electrode system in a 1.0 M KOH electrolyte. Figure 5(a) depicts the CV curves of the various carbon electrodes at a scan rate of 10 mV/s. The PC-4K-CO_2 sample displayed the highest CV-circulated area and thus the highest specific capacitance among all the tested samples at a scan rate of 10 mV/s, as shown in Figure 5(a). This finding is consistent with the aforementioned material characterization data. All the tested porous carbon electrodes showed a rectangular-like CV curve, reflecting their good capacitive behavior as supercapacitor electrode materials. By comparing the rectangular CVs of the tested electrodes in Figure 5(a), it is evident that all of the CVs maintained the rectangular shape with no major deviation. Due to the presence of numerous oxygen-containing functional groups, PC-4K-N_2, PC-5K-CO_2, and PC-6K-CO_2 may undergo some degree of redox reaction in the KOH electrolyte, increasing the leakage current of the capacitor. This is indicated by the small and asymmetrical current peak on the right side of the collected CVs (between -0.1V and 0.2V region) (Figure S3). The rectangular-shaped CV curve and good symmetry represent the typical double-layer capacitance of the electrode. This is also an indication of its high-rate capability and excellent electrochemical reversibility. This implies good charge propagation and quick ion diffusion in all of the electrodes at a 10 mV/s scan rate. The high rate performance favors the delivery of both high power density and high energy density. The rate-dependent CV curves of PC-4K-CO_2 with the scan rates from 20 to 500 mV/s are illustrated in Fig. 5(b). The rectangular shape CVs, especially seen at 20 mV/s and 50 mV/s, are indicative of typical supercapacitor behavior. The departure of the CV curves from the rectangular shape grows when the scan rate is gradually raised, caused by the high degree of electrochemical polarization.

Fig. 5(c) shows comparative charge-discharge curves for the PC-CO_2, PC-4K-CO_2 and PC-4K-N_2 pistachio shell-derived porous carbon electrodes at a current density of 0.5 A/g. All of these samples displayed GCD profiles that were nearly triangular, indicating good charge storage as a result of the correct development of electrical double layers at the interfaces. Based on Equation (1), the gravimetric specific capacitances of PC-CO_2, PC-4K-CO_2, PC-5K-CO_2, PC-6K-CO_2 and PC-4K-N_2 were calculated to be 0.65, 151, 90, 75 and 70 F/g, respectively, at a current density of 0.5 A/g. The as-prepared porous carbon electrodes displayed a gravimetric specific capacitance in the following order: PC-4K-CO_2 > PC-5K-CO_2 > PC-6K-CO_2 > PC-4K-N_2> PC-CO_2 in 1 M KOH electrolyte solution (Figure 5c and Figure S4). The higher gravimetric specific capacitance of the PC-4K-CO_2 sample in terms of its KOH ratio (wt. ratio of biochar/KOH of 1/4) and the activation in the CO_2 gas environment can be attributed to its more advanced microporous structures, which are conducive to the

adsorption and transport of ions. Despite having the same KOH content, the better electrochemical performance of the PC-4K-CO_2 sample than the PC-4K-N_2 sample is due to its higher microporous structure which resulted from the physical activation using the CO_2 gas and its excellent surface properties. Figure 5(d) shows the GCD curves of the pistachio shell-derived porous carbon sample (PC-4K-CO_2) at the current density ranging from 1 to 20 A/g. A very small IR drop (at the beginning of the discharge curve) was observed in the symmetrical triangular curves at different specific currents, which is also in agreement with Figure 5(d). The absence of significant voltage drop (IR) in linear symmetric GCD curves indicates that the electrochemical performance of the obtained materials is highly reversible. In the literature review summarized in Table 2, the performance comparison of present work with reported biomass-derived porous activated carbon electrodes for supercapacitor applications was compared and showed that PC-4K-CO_2 electrode was effective for supercapacitor applications.

Electrochemical impedance spectroscopy (EIS) analysis of PC-4K-CO_2 and PC-4K-N_2 samples are given in Figure 5(e) and all samples are given in Figure S5. EIS was examined over a frequency range of 0.01 Hz–100 kHz and at a voltage of 5 mV open circuit to assess the electrochemical behavior of supercapacitors. In addition to the internal resistance of the current collector, the internal resistance (R_e) of the electrode material, including the electrode and the contact resistance between them, determines the intersection of the EIS curve on the X-axis. The charge transfer resistance (R_{ct}) affected by the electrical double-layer structure is represented by the radius of the semicircle in the high-frequency region. Compared to the other electrodes, the electrode with the lowest charge transfer resistance (R_{ct}) indicated by the diameter of the semicircle belongs to the PC-4K-CO_2 sample.

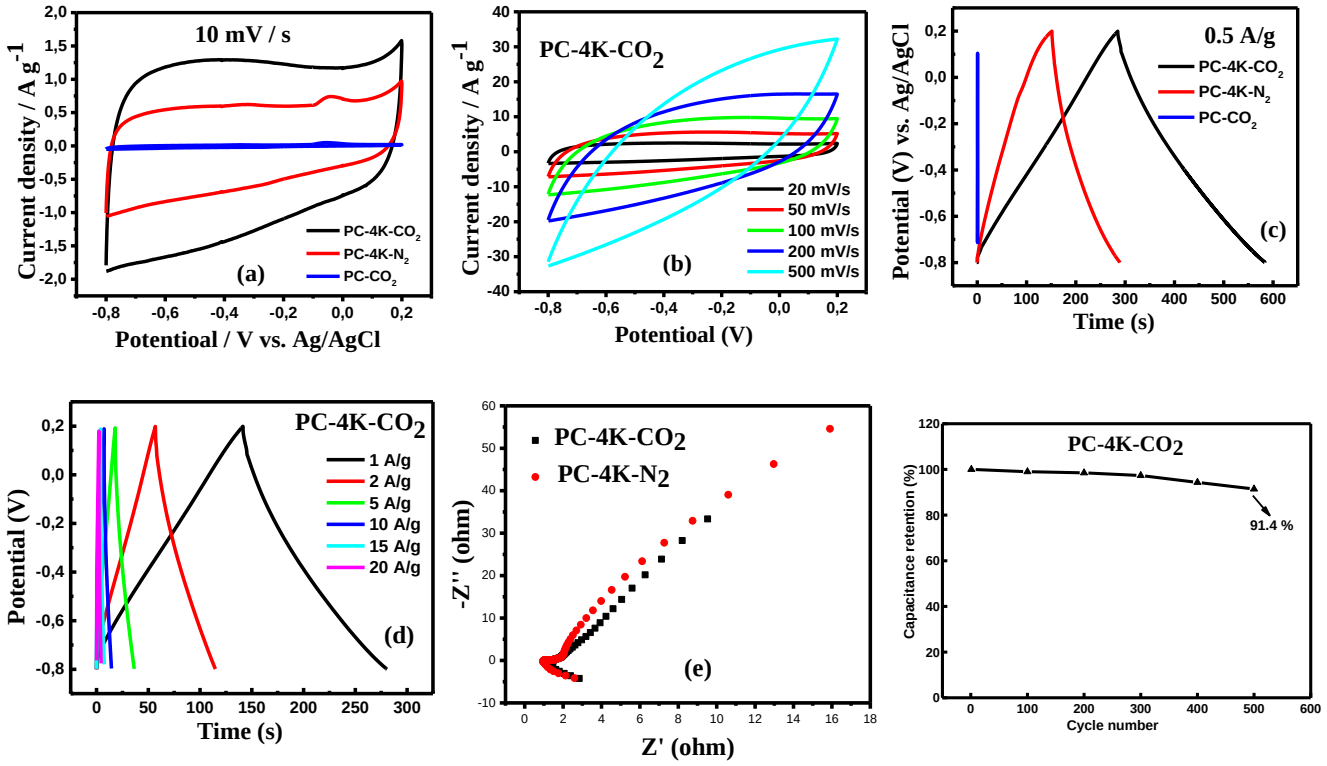

Figure 5. Cyclic voltammograms of PC-CO_2; PC-4K-CO_2 and PC-4K-N_2 measured a) at 10 mVs^{-1} for these samples b) from 20 to 500 mVs^{-1} for PC-4K-CO_2 in 1M KOH, the GCD curves (c) for PC-CO_2; PC-4K-CO_2 and PC-4K-N_2 samples at a current density of 0.5 A/g (d) PC-4K-CO_2 at current densities from 1 to 20 A/g in the three-electrode system, Nyquist plots of PC-4K-CO_2 and PC-4K-N_2 electrodes (e) cycling retention

In addition, the R_s value represented by the X-intercept on the graph is also the lowest for the PC-4K-CO_2 sample. This confirms the high electrical conductivity of the PC-4K-CO_2 electrode. When Nyquist curves revealed by electrochemical impedance spectroscopy analyzes are examined, it is seen that the results obtained in GCD and CV analyses are supportive. It is seen that PC-4K-CO_2 and PC-4K-N_2 samples have a similar graphic appearance to the typical ultracapacitor Nyquist curve shown in Figure 5(e), except for the porous carbon sample coded PC-CO_2 (Figure S5). When all sample curves are considered, it is seen that the PC-4K-CO_2 sample exhibited more ideal capacitive performance and higher electrochemical performance than the other samples. Chronopotentiometry testing at a constant current density of 5 A/g up to 500 cycles is used to assess the cycling durability of PC-4K-CO_2 (Fig. 5f). It has been observed that the PC-4K-CO_2 electrode displays cycle stability with less than 8.6% capacitance decline after 500 continuous cycles, indicating improved electrochemical stability. There are two main factors affecting the specific capacitance and energy density of the porous materials. The first one is the surface textural properties including surface area, pore size distribution etc. The second one is the surface functionality of the carbon-based material. (Sun et al., 2023; Farshadnia, 2023).

Table 2. Performance comparison of present work with reported biomass-derived porous activated carbon electrodes for supercapacitor applications

Biomass	Activation Method	Electrolyte	Specific capacitance (F/g)	Current density (A/g)	References
Coconut shell	Physical activation	6.0 M KOH	192	1.0	(Yaokang et al., 2012)
Baby-diaper	Physical activation	1.0 M H_2SO_4	81	0.5	(Mi et al., 2012)
Banana peel	Chemical activation	6.0 M KOH	206	1.0	(Wang et al., 2015)
AC derived from *Quercus suber*	Chemical activation	1.0 Na_2SO_4	166	0.5	(Lu et al., 2016)
AC from platanus fruit	Chemical activation	1.0 M H_2SO_4	223	0.5	(Yang et al., 2017)
AC from platanus fruit	Chemical activation	1.0 M H_2SO_4	223	0.5	(Yang et al., 2017)
Wallnut shell	Chemical activation	6.0 M KOH	263	0.5	(Faaith et al., 2017)
AC from walnut shell	Chemical activation	6.0M KOH	186.7	0.5	(Zhao et al., 2018)
AC from bamboo shells	Chemical activation	1.0 M H_2SO_4	181	0.5	(Sesuk et al., 2019)
Rose	Chemical activation	6.0 M KOH	208	0.2	(Gandla et al., 2020)
Porous carbon from cattail biomass	Physical activation	6.0 M KOH	126.5	0.5	(Fu et al., 2020)
AC from coconut coir pith	Chemical activation	1.0 M H_2SO_4	202	0.5	(Huang et al., 2021)
Pistachio Shell-derived PS	Chemical and Physical activation	1.0 M KOH	151	0.5	(This work)

CONCLUSION

To summarize, pistachio shell biomass has been utilized to produce porous carbons activated by a combination of KOH and CO_2. The obtained products showed a sponge-like morphology with a large number of mesopores and micropores. This type of hierarchical porous structure is of great importance in terms of facilitating charge transport and providing sufficient active space for energy storage applications. Among all the tested products, the PC-4K-CO_2 sample has the highest surface area which contributes to the best performance as the electrode material for supercapacitors. Therefore, we conclude that the samples obtained by simultaneous use of chemical activation (Pistachio Shell/KOH:1/4) and physical activation (using CO_2) may be more suitable for supercapacitor applications of porous carbons derived from pistachio shells. At a current density of 0.5 A/g, PC-4K-CO_2 coded samples were used as the electrode material to achieve the highest specific capacitance of 151 F/g. Besides, the electrode prepared with PC-4K-CO_2 sample has achieved an excellent long-cycling life with only an 8.6% loss of its initial capacitance over 500 cycles even at 5 A/g. As a result, biochar materials from natural resources such as pistachio shells can be turned into valuable electrode materials for energy storage devices.

ACKNOWLEDGEMENTS

This project was supported by The Scientific and Technological Research Council of Türkiye (TUBITAK) through Project TEYDEP 2200261 and The Scientific Research Council of Osmaniye Korkut Ata University through project 2020-PT2-002. The authors also thank MSLM27 Technology Development and Consulting Company for their financial and consultancy support.

Conflict of Interest

The article authors declare that there is no conflict of interest between them.

Author's Contributions

The authors declare that they have contributed equally to the article.

REFERENCES

Ahmadpour A., Do, DD,. (1996). The preparation of active carbons from coal by chemical and physical activation.Carbon, 34(4), 471-479.

Ahmadpour, A., King, B. A., Do, DD,. (1998). Comparison of equilibria and kinetics of high surface area activated carbon produced from different precursors and by different chemical treatments. Industrial & Engineering Chemistry Research, 37(4), 1329-1334.

Altay, B. N., Aksoy, B., Banerjee, D., Maddipatla, D., Fleming, P. D., Bolduc, M., Demir, M., (2021). Lignin-derived carbon-coated functional paper for printed electronics. Acs Applied Electronic Materials, 3(9), 3904-3914.

Altinci, O. C., Demir, M., (2020). Beyond conventional activating methods, a green approach for the synthesis of biocarbon and its supercapacitor electrode performance. Energy & Fuels, 34(6), 7658-7665.

Ashourirad, B., Demir, M., Smith, R. A., Gupta, R. B., El-Kaderi, H. M., (2018). Rapid transformation of heterocyclic building blocks into nanoporous carbons for high-performance supercapacitors. Rsc Advances, 8(22), 12300-12309.

Beihu Lu, L. H., Huayi, Y., Xuhui, M., Wei, X., Dihua, W., (2016). Preparation and application of capacitive carbon from bamboo shells by one step molten carbonates carbonization. International journal of hydrogen energy, 41, 18713-18720.

Chen, J., Zhou, X., Mei, C., Xu, J., Zhou, S., Wong, C..P., (2017). Evaluating biomass-derived hierarchically porous carbon as the positive electrode material for hybrid Na-ion capacitors. Journal of Power Sources, 342, 48-55.

Chongjun, Z. Y. H., Chunhua, Z., Xiaoxiao, S., Zhaoqiang, Z., (2018). Rose-derived 3D carbon nanosheets for high cyclability and extended voltage supercapacitors. Electrochimica Acta, 291, 287-296.

Choudhury, F. A., Norouzi, N., Amir, K., Demir, M., El-Kaderi, H. M., (2021). Iron-based sulfur and nitrogen dual doped porous carbon as durable electrocatalysts for oxygen reduction reaction. International Journal of Hydrogen Energy, 47, (9), 6078-6088

Demir, M., Jethrine, B. A., Mugumya, H. K., Sushil, H., El-Kaderi, S., Gupta, M. B. R., (2018). Nitrogen and oxygen dual-doped porous carbons prepared from pea protein as electrode materials for high performance supercapacitors. International journal of hydrogen energy, 43, 18549-18558.

Du, W., Wang, X., Sun, X., Zhan, J., Zhang, H., Zhao, X., (2018). Nitrogen-doped hierarchical porous carbon using biomass-derived activated carbon/carbonized polyaniline composites for supercapacitor electrodes. Journal of Electroanalytical Chemistry, 827, 213-220.

Duan, F., Zhang, J. P., Chyang, C. S., Wang, Y. J., Tso, J., (2014). Combustion of crushed and pelletized peanut shells in a pilot-scale fluidized-bed combustor with flue gas recirculation. Fuel Processing Technology,128, 28-35.

Faith, O., Ochai-Ejeh, A. B., Julien, D., Abubakar, A. K., Moshawe, J. M., Farshad, B., Ncholu, M., (2017). High electrochemical performance of hierarchical porous activated carbon derived from lightweight cork (Quercus suber). Journal of Mater Science: Mater Electron, 52, 10600-10613.

Fan, M., Marshall, W., Daugaard, D., Brown, R. C., (2004). Steam activation of chars produced from oat hulls and corn stover. Bioresource Technology, 93(1), 103-107.

Farshadnia, M., Ensafi, A. A., Mousaabadi, K. Z., Rezaei, B., Demir, M., (2023). Facile synthesis of NiTe2-Co2Te2@rGO nanocomposite for high-performance hybrid supercapacitor. Scientific Reports, 13, 1364.

Gandla, D., Chen, H., Tan, D. Q., (2020). Mesoporous structure favorable for high voltage and high energy supercapacitor based on green tea waste-derived activated carbon. Materials Research Express, 7(8).

Gao, Y., Zhou, Y. S., Qian, M., He, X. N., Redepenning, J., Goodman, P., Lu, Y. F., (2013). Chemical activation of carbon nano-onions for high-rate supercapacitor electrodes. Carbon, 51, 52-58.

Girgis, B. S., Soliman, A. M., Fathy, N.A. (2011). Development of micro-mesoporous carbons from several seed hulls under varying conditions of activation. Microporous and Mesoporous Materials,142(2-3), 518-525.

Guo, F., Jiang, X., Li, X., Peng, K., Guo, C., Rao, Z. (2019). Carbon electrode material from peanut shell by one-step synthesis for high performance supercapacitor. Journal of Materials Science: Materials in Electronics, 30(1), 914-925.

Hai-Hai, F. L. C., Haojie, G., Xiaokun, Y., Juan, H., Gang, W., Feng, Y., Haoquan, L., Changchun, F., Yu-Lin, S., Xuhong, G., (2020). Walnut shell-derived hierarchical porous carbon with high performances for electrocatalytic hydrogen evolution and symmetry supercapacitors. International journal of hydrogen energy, 45, 443-451.

Huafang, Y. Y. T., Xiaogu, H., Lixi, W., Qitu, Z. (2017). Activated porous carbon derived from walnut shells with promising material properties for supercapacitors. Journal of Mater Science: Mater Electron, 28, 18637-18645.

Huang, Y. G., Wang, Y. Y., Cai, Y. Z., Wang, H. Q., Li, Q. Y., Wu, Q., Ma, Z. L. (2021). Diatomite waste derived N-doped porous carbon for applications in the oxygen reduction reaction and supercapacitors. Nanoscale Advances, 3(13), 3860-3866.

Inagaki, M., Konno, H., Tanaike, O. (2010). Carbon materials for electrochemical capacitors. Journal of Power Sources,195(24), 7880-7903.

Juan, M., X-R, W., Rui-Jun, F., Wen-Hui, Q., Wen-Cui, L. (2012). Coconut-shell-based porous carbons with a tunable micro/ mesopore ratio for high-performance supercapacitors. Energy & Fuels, 26, 5321-5329.

Kalyani, P., Anitha, A. (2013). Biomass carbon & its prospects in electrochemical energy systems. International Journal of Hydrogen Energy, 38(10), 4034-4045.

Li, N., Yue, Q., Gao, B., Xu, X., Su, R., Yu, B. (2019). One-step synthesis of peanut hull/graphene aerogel for highly efficient oil-water separation. Journal of Cleaner Production, 207, 764-771.

Miller, J. R., Simon, P. (2008). Electrochemical capacitors for energy management. Science, 321(5889), 651-652.

Mingyang, Z. Y. S., Rongjun, S. (2021). Hierarchical porous carbon obtained by Mg–Al double hydroxide templates with high volumetric capacitance and rate performance. Microporous and Mesoporous Materials, 330, 111593-111601.

Mousavi, S.S., Nasrollahzadeh, B. J. M., Eslamipanah, M., Khazalpour, S., Orooji, Y. (2021). Laser-assisted synthesis of bentonite/Pd nanocomposite and its electrochemical hydrogen storage capacity. Microporous and Mesoporous Materials, 328, 111439-111449.

Sesuk, T., Jivaganont, P. T. P., Somton, K., Limthongkul, P., Kobsiriphat, W. (2019). Activated carbon derived from coconut coir pith as high performance supercapacitor electrode material. Journal of Energy Storage, 25, 100910-100919.

Sun, Y., Xue, S., Sun, J., Li, X., Ou, Y., Zhu, B., Demir, M. (2023). Silk-derived nitrogen-doped porous carbon electrodes with enhanced ionic conductivity for high-performance supercapacitors. Journal of Colloid and Interface Science

Wei, D., Chen, Z., Jin, J., Wei, B., Li, Q., Yang, S.,Wang, X. (2018). Interaction of U (VI) with amine-modified peanut shell studied by macroscopic and microscopic spectroscopy analysis. Journal of Cleaner Production, 195, 497-506.

Williams, P. T., Reed, A. R. (2006). Development of activated carbon pore structure via physical and chemical activation of biomass fibre waste. Biomass and Bioenergy, 30(2), 144-152.

Xiaodu, L, R, L., Xiaoliang, W. (2021). Biomass waste derived functionalized hierarchical porous carbon with high gravimetric and volumetric capacitances for supercapacitors. Microporous and Mesoporous Materials, 310, 110659-110666.

Xin, W. Z. G., Jiuli, C., Dapeng, W., Xiaorui, W., Fang, X., Yuming, G., Kai, J. (2015). Electrochemical energy storage and adsorptive dye removal 5 of platanus fruit derived porous carbon. RSC Advances, 5, 15969-15976.

Yaokang, L. L. G., Mingxian, L., Wei, X., Zijie, X., Dazhang, Z., Dominic, S. W. (2012). A self-template synthesis of hierarchical porous carbon foams based on banana peel for supercapacitor electrodes. Journal of Power Sources, 209, 152-157.

Yu, K., Zhu, H., Qi, H., Liang, C. (2018). High surface area carbon materials derived from corn stalk core as electrode for supercapacitor. Diamond & Related Materials, 88, 18-22.

Zhan, Y., Zhou, H., Guo, F., Tian, B., Du, S., Dong, Y., Qian, L. (2021). Preparation of highly porous activated carbons from peanut shells as low-cost electrode materials for supercapacitors. Journal of Energy Storage, 34, 102180.

Zhang, L. L., Zhao, X.S. (2009). Carbon-based materials as supercapacitor electrodes. Chemical Society Reviews, 38(9), 2520-2531.

Zhang, S., Shi, X., Wróbel, R., Chen, X., Mijowska, E. (2019). Low-cost nitrogen-doped activated carbon prepared by polyethylenimine (PEI) with a convenient method for supercapacitor application. Electrochimica Acta, 294, 183-191.

Zhang, T., Walawender, W. P., Fan, L., Fan, M., Daugaard, D., Brown, R. C. (2004). Preparation of activated carbon from forest and agricultural residues through CO2 activation. Chemical Engineering Journal, 105(1-2), 53-59.

Zhang, X., Jiao, Y., Sun, L., Wang, L., Wu, A., Yan, H., Fu, H. (2016). GO-induced assembly of gelatin toward stacked layer-like porous carbon for advanced supercapacitors. Nanoscale, 8(4), 2418-2427.

Zhao, J., Li, Y., Huang, F., Zhang, H., Gong, J., Miao, C., Zhu, K., Cheng, K., Ye, K., Yan, J., Cao, D., Wang, G., Zhang, X. (2018). High-performance asymmetric supercapacitor assembled with three-dimensional, coadjacent graphene-like carbon nanosheets and its composite. Journal of Electroanalytical Chemistry, 823, 474-481.

Zhao, L., Fan, L. Z., Zhou, M. Q., Guan, H., Qiao, S., Antonietti, M., Titirici, M. M. (2010). Nitrogen-containing hydrothermal carbons with superior performance in supercapacitors. Advanced Materials, 22(45), 5202-5206.

Zhong, X. X., Mao, Q. Y., Li, Z. S., Wu, Z. G., Xie, Y. T., Li, S. H., Wang, H. Q. (2021). Biomass-derived O, N-codoped hierarchically porous carbon prepared by black fungus and Hericium erinaceus for high performance supercapacitor. Rsc Advances, 11(45), 27860-27867.